Lithospheric thickness under the Dinarides

Tena Belinić[a], Josip Stipčević[a,*], Mladen Živčić[b], and the AlpArrayWorking Group[**]

[a]*Department of Geophysics, Faculty of Science, University of Zagreb, Horvatovac 95, 10000 Zagreb, Croatia*
[b]*Slovenian Environment Agency, Vojkova 1b, SI-1000 Ljubljana, Slovenia*

Abstract

The nature of the interaction between Adriatic and Euroasian lithospheric plates in the Dinarides is important for understanding the complex tectonic history of the central Mediterranean. Using the data from permanent and temporary seismic stations in the wider Dinaric region, we imaged the lithospheric and upper mantle structure under this area. Specifically, we focused on mapping the lithosphere asthenosphere boundary (LAB) using the S receiver functions in order to establish boundaries between different tectonic domains present in this region. The lithospheric thickness in the investigated area varies between ∼50 and ∼160 km with high degree of variability between adjacent tectonic realms. Below northwestern Dinarides the LAB depth varies between 100 and 120 km thinning towards Adriatic sea and Pannonian basin, to 90 and 70 km respectively. In the central Dinaric region (Lika region) we find anomalously thin lithosphere with thickness varying between 50 and 70 km and weak velocity gradient defining the LAB. Further south the signal from the LAB is more pronounced with lithosphere

*Corresponding author
**www.alparray.ethz.ch
Email address: `jstipcevic@gfz.hr` (Josip Stipčević)

getting thicker again with average depths around 90 km. The intriguing observation of thinned lithosphere under central part of the Dinarides coincides with the zone of lower seismicity and with the tomographic images showing the slab gap in this area.
Keywords:

Lithoshpere-asthenosphere boundary, Receiver functions, Dinarides

---

1. Introduction

Interaction between the Adriatic microplate (Adria) and stable Europe played the vital role in the shaping of the Central Mediterranean. Although many papers have been written about Adria, most of them deal with the northern and western margins of Adria (i.e. Alps and Apennines) with relatively few exploring the northeastern boundary zone in the Dinarides. The Dinarides are the trust and fold belt located roughly between the Adriatic Sea and the Pannonian basin (Fig. 1). Their formation started in the Middle-Late Jurassic with the progressive closure of the Neotethyan ocean (Pamić et al., 1998; Schmid et al., 2008; Handy et al., 2015). Northward movement of Adria, then still part of the African plate, initiated the subduction along the Dinaric margin which probably lasted until Late Cretaceous-early Paleogene time when it was replaced by the collision (Pamić, 2002; Schmid et al., 2008; Ustaszewski et al., 2010). Collisional shortening in the Dinarides, where Adria is the compliant lower plate, was accompanied by the nappe stacking and folding of the Adria's carbonate platform. This produced a thick carbonate sedimentary cover at places reaching thickness in excess of 10 km (Aljinović, 1983). Shaping of the Dinarides was also influenced by the neighbouring tectonic processes like the extension in the Pannonian basin and the extrusion in the Eastern Alps (Ratschbacher et al., 1991b,a; Schmid et al., 2008; Ustaszewski et al., 2008; Neubauer, 2014).

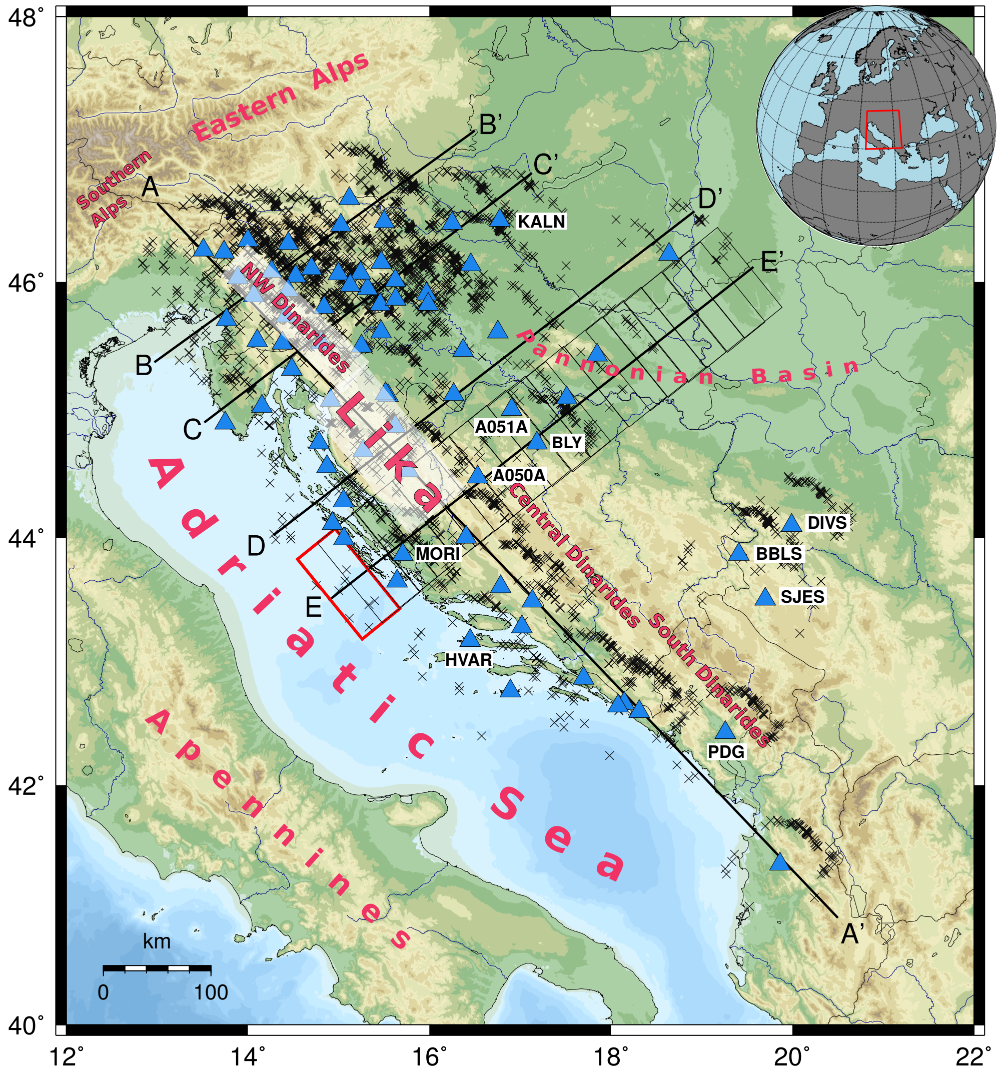

Figure 1: Map of the wider Dinarides area with seismological stations (blue triangles) used in this study. Names of the several stations mentioned in the main text are marked. The inset shows the study area location in the central Mediterranean. Black lines indicate the location of the cross sections used in the research along with the SRF piercing points at 90 km depth (black crosses).

The long history of the interaction between Adria and Europe can be pieced together from the teleseismic tomographic images by tracing positive velocity anomalies under the mountain chains surrounding the Adriatic Sea. Beneath the Western and the Central Alps tomography maps south-easterly dipping slab consistent with the south-southeast directed subduction of the Alpine Tethys (Bijwaard and Spakman, 2000; Wortel, 2000; Piromallo and Morelli, 2003) while the orientation of the slab below the Eastern Alps is more controversial with results pointing either to the southward (Piromallo and Morelli, 2003) or northward (Lippitsch, 2003) directed subduction. The question of the slab orientation under the Eastern Alps is especially important in the scope of Dinaric research as each distinct orientation draws different conclusions about the geodynamical processes under the Dinarides. Southward oriented subduction fits well with the overall image of the Alpine-Carpathian orogenesis where the European continental lower lithosphere was subducted below the Adria along the whole Europe-Adria boundary. In this scenario Alpine and Dinaric subduction-collision systems are two distinct entities and interaction between them and the Pannonian Basin is regulated through a triple junction point mechanism (Brückl et al., 2007, 2010). On the other hand, northward oriented subduction is compatible with the images of a northeast dipping slab along the active Hellenic arc-trench system which extends to the Central and Southern Dinarides (Bijwaard and Spakman, 2000; Piromallo and Morelli, 2003). Recently, Handy et al. (2015) proposed a hypothesis in which the southward dipping subduction under the Eastern Alps was replaced by the north oriented subduction of the Adriatic lithosphere following the slab brake-off. In this context it is important to highlight an even more unusual anomaly that keeps appearing on regional tomographic images: a large negative velocity anomaly beneath the central part of the Dinarides (Bijwaard and Spakman, 2000; Wortel, 2000; Lippitsch, 2003; Piromallo and Morelli, 2003; Koulakov et al., 2009;

Mitterbauer et al., 2011). This anomaly separates the aforementioned lithosphere slab anomaly in the Eastern Alps from the positive anomaly mapped beneath the southern portion the Dinarides, and it is somewhat unexpected due to significant thrust shortening. Ustaszewski et al. (2008) proposed an explanation for this slab gap: thermal erosion of the Adriatic lithospheric slab due to the opening of the Panonnian basin and an influx of the hot asthenospheric material. On the other hand, in the model of Handy et al. (2015) the slab gap evolved on the foundation of the former transfer fault (Alps–Dinarides Transfer Fault or ADT2 in Handy et al. 2015) linking the opposing Alpine and Dinaric subduction systems. The Alps-Dinarides Transfer Fault was active until around 20-23 Ma and was later overprinted by the subsequent tectonic activity (e.g. Miocene clockwise rotation and strike-slip faulting in the Pannonian basin). This model combines slab tearing beneath the Alps and the Dinarides, northward movement and subduction of Adria beneath the Eastern Alps (for details we refer the reader to the paper of Handy et al. 2015). In addition, there are suggestions that part of the extension in Panonnian basin can be attributed to the delamination and slab rollback under the Dinarides (Schefer et al., 2011; Matenco and Radivojević, 2012). This hypothesis is interesting as it means that the slab gap could have developed due to the strong asthenospheric corner flow around the northern edge of the sinking slab.

Another important question arising from the teleseismic tomographic images is the nature of the interaction between Adria and European mainland beneath the Central and the Southern Dinarides. Observations show a shallow high velocity anomaly under this area reaching up to 200 km depth (Bijwaard and Spakman, 2000; Wortel, 2000; Piromallo and Morelli, 2003; Koulakov et al., 2009). Most interpretations agree that this anomaly represent underthrusting of the continental

Adria lithosphere beneath the Dinarides (Ustaszewski et al., 2008; Schmid et al., 2008; Ustaszewski et al., 2010; Handy et al., 2015; Šumanovac, 2015). As already mentioned, Matenco and Radivojević (2012) have taken their interpretation a bit further by suggesting collisional subduction accompanied by the slab roll-back. By modelling global positioning system measurements of crustal velocity along a profile crossing the south-central Dinarides Bennett et al. (2008) have found evidence for an ongoing subduction in the southern Adriatic.

During the last decade, most of the research done in the Dinarides was concentrated on the crust whilst trying to reconcile surface geology data with the results from geophysical investigations. Several studies mapped crustal thickness in the area with general agreement of the thicker crust under the Dinarides ($\sim$ 40 km) thinning towards the Pannonian Basin and the Adriatic Sea (Skoko et al., 1987; Šumanovac et al., 2009; Stipčević et al., 2011). Combining gravity and seismic data on a profile crossing the northwestern Dinarides Šumanovac et al. (2009) identified a two-layer Dinaridic crust: upper crust with lower P-wave velocity ($\sim$ 6 km/s) and lower crust with velocities ranging between 6.5 and 7.1 km/s); and a single layered Panonnian crust. However, till now, there were no large scale studies of the lithospheric thickness under the Dinarides and the depth of the lithospheric-asthenospheric boundary (LAB) is largely unknown. Geissler et al. (2010) found that the typical continental lithosphere beneath central Europe has thickness of about 80-110 km, including the several stations in the Panonian Basin ($\sim$ 80 km). Bianchi et al. (2014) estimated the depth of LAB beneath the central Eastern Alps at around 120–130 km which shallows towards west to approximately $80 - 90$ km. Also, they found lithospheric thinning towards the Pannonian Basin (down to $70 - 80$ km) that supports the premise about the lateral extrusion.

In this paper, our aim is to investigate the lithospheric thickness distribution under the Dinarides, discuss the implications of our findings on the geodynamic processes in the region and compare our measurements to the results from the previous investigations. This will provide valuable clues to decipher geodynamics that shaped the Central Mediterranean area and help us understand the driving forces behind the current tectonic processes. For this purpose we use the S-wave receiver function method (SRF) on a number of teleseismic events recorded on all the available seismic stations in the wider Dinarides area.

2. Data and methods

We collected seismic waveform data from 74 seismic stations (Fig. 1) most of which belong to the Croatian Seismic Network (CSN) and the Slovenian Environment Agency (ARSO), 31 and 28 respectively, with 6 additional stations coming from the AlpArray temporary network (Molinari et al., 2016), 5 from the Mediterranean Network (MedNet), 2 from the Hungarian National Seismological Network and 2 from the Serbian Network of Seismic Stations. Majority of the used data was recorded in the period between 2010 and the end of 2016 with the exception of AlpArray stations which were deployed in 2015 and 2016. For this set of stations we managed to collect more than 12844 waveforms from 270 events with magnitude (Mw) greater than 6.0 at distances of $55° - 85°$. At these distances most of the suitable events are located in the western Pacific seismic zone stretching from Kamchatka to Indonesia, which results in the better sampling of the North-Eastern quadrant around each station (Fig. 1).

During the last decade S receiver function method has slowly emerged as one of the most effective tools in detection of the upper mantle discontinuities and transition zones (Abt et al., 2010; Geissler et al., 2012; Levander and Miller, 2012; Bianchi et al., 2014; Shen et al., 2017). The SRF method isolates the S-to-P (Sp) converted waves generated from the incoming teleseismic S-waves passing through seismic discontinuities (Farra and Vinnik, 2000; Yuan et al., 2006). This approach has been particularly successful in mapping the lithosphere-asthenosphere boundary (LAB). Because the Sp phase arrives earlier then the incident S wave the SRFs are not contaminated by the multiples which is a common problem when using the P receiver function (PRF) to explore the LAB. Due to strong S-wave attenuation in the mantle, the SRFs contain lower frequencies than PRFs, which results in lower spatial resolution than is the case with converted P-waves attenuation in the mantle. This makes the SRFs more appropriate for gradual transition zones, like the LAB, whereas the higher frequency PRFs are usually used to map sharp impedance contrasts in the crust and uppermost mantle. According to Yuan et al. (2006), LAB can be seen at distances between $55°$ and $85°$ with maximum amplitudes at $60° - 70°$. The upper distance limit exists because of the arrival of strong SKS and SKSp waves and their interference with the arrival of mantle S waves, while the lower distance limit depends on the depth of the discontinuity we are exploring, in our case in the uppermost mantle. In addition, at smaller distances S wave incidence angle is postcritical (Wilson et al., 2006) which means that there is no converted Sp waves because the S wave incidence angle is larger than $45°$.

Before calculating SRFs we visually inspected all traces and retained only those with clear S-wave arrivals and with the signal-to-noise ratio larger than 3. The final number of waveforms per station varied depending on the noise and station operational duration. For some stations, most notably recently installed

AlpArray ones, only a few usable waveforms were found while for other stations we were able to collect over a hundred quality traces. To calculate the SRFs, we broadly followed the steps outlined in Kind et al. (2012). Firstly, all the selected waveforms were cut 100 s before and 20 s after the S-phase arrival which is taken as the time origin. Time axes of the waveforms were then reversed, so that the Sp conversion arrival time is positive. After removing the mean and trend, we transform the data from the usual vertical, north-south and east-west (ZNE) components, into the ray coordinate system (LQT). This transformation was performed using the theoretical backazimuth of each event and the incidence angle determined by the minimization of the L component at the time of the S-wave arrival. In theory, the Q component should contain only the SV-wave amplitudes while the Sp phases will mostly dominate the L component.

Next, the deconvolution was performed to source normalize the waveforms and remove the residual S wave signal from the L component. The L component is deconvolved with the Q component in time domain using the iterative deconvolution approach (Ligorría and Ammon, 1999) which is based on the least-squares difference minimization between the observed L component and the predicted signal. Similarly to the time axis reversal, the amplitudes were reversed in order to keep waveform appearance consistent with the P receiver functions. We retained only the SRFs with the peak amplitudes in the range $0.001 - 1.0$ (Yang et al., 2016) and with the iterative deconvolution fit above 85%. Finally, we visually inspected all the receiver functions to discard noisy and anomalous waveforms thus obtaining our consolidated receiver function set.

Usually, the Sp converted phases are difficult to notice on a single seismogram since only a small percentage of the incident energy is converted. Because of this, a number of records must be summed to enhance these phases and highlight the local structure beneath the receiver. Here we perform two different styles of summation, station summation and common conversion point stacking (Dueker and Sheehan, 1997). Station summation consist of stacking all the moveout corrected receiver functions recorded at one station (Fig. 2). Moveout correction was done to a reference slowness of 6.4 s/deg using the IASP91 1D velocity model (Kennett, 1991). In this way we are left with an average SRF representing the structure around the receiver. For deep discontinuities, like the LAB, sampling distance offset from the receiver will be significant, and by station averaging we may lose some information about lateral variation. Nevertheless, station SRF stack provides good approximation of the structure beneath the receiver, and gives valuable information about lithospheric thickness there. Station stacks are depth-converted using the IASP91 model which is appropriate for determining the LAB depth, even in complex surroundings (Miller and Eaton, 2010; Zhai and Levander, 2011; Levander and Miller, 2012). In Fig. 2 we show examples of the S receiver functions from two stations situated in the different tectonic domains. Station KALN is situated in the Pannonian basin whereas MORI station is located in the contact zone between the Adriatic and the Dinarides. Positive amplitudes are marked with blue while negative values are colored in red. At both stations the Moho phase (SMp) is clearly visible as the strong positive amplitude arriving between 3 and 5 seconds while the phase converted at the LAB is more subtle and can be seen as the wider negative signal arriving after the Moho phase.

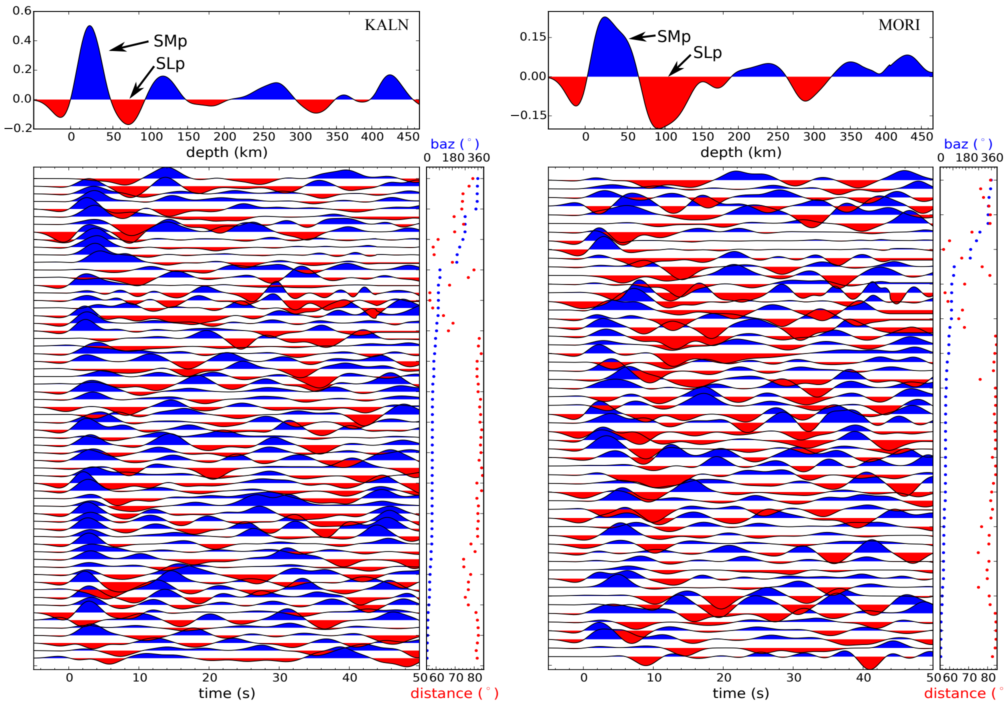

Figure 2: Moveout-corrected S receiver functions sorted by backazimuth at stations KALN (left) and MORI (right) (locations in Fig. 1). Blue and red lobes represent positive and negative energy, respectively. The stacking results are shown in the top panels and panels on the right show distance (red dots) and backazimuth (blue dots) of each receiver function. Stacked SRFs shown in the top panel are depth converted and Moho and LAB phases are marked with SMp and SLp, respectively.

To further explore lateral structural variation in the study area we use the Common Conversion Point stacking (CCP) on one orogen-parallel profile (AA', see the location of in Fig. 1). Using the CCP stack along this profile we are able to show finer scale lateral variations and emphasize structural differences along the Dinarides. To create CCP sections, locations of piercing points of Sp phase at a depth of 90 km (Sp90) are first calculated for all the events using the IASP91 model. Then, area along the profile is divided into rectangular boxes where each box has a 50%

overlap with the neighbouring boxes. For each box, an average SRF is created by stacking individual traces with respective Sp90 piercing points within the box boundaries. The size of the boxes along this profile (AA') is chosen to be 40 km $\times$ 80 km (length along the profile $\times$ width) which was large enough to collect an average of 40 SRFs per box. As with the station stacking all traces were moveout corrected to a reference slowness of 6.4 s/deg before stacking. Finally, as each of the box averaged traces represents one point along the profile, after the depth conversion we are left with the image of seismic structure along the profile.

3. Results

Using the SRF techniques outlined in the previous section we examine the negative amplitude signals arriving after the strong positive Moho phase (see Fig. 2). These negative amplitudes are linked to the negative impedance contrast generated by an interface in the upper mantle. In Fig. 3 we show all the depth converted SRF station stacks ordered by the increasing depth of the negative amplitude phase associated with the LAB. The appearance of this phase in our results varies from sharp, almost pulse like, to the more diffused, stretched, multi-peak signal. While the Moho phase is usually seen as sharp positive signal associated with the rapid increase in seismic velocity, variable nature of the LAB phase hints that this transition zone is not as homogeneous as is the crust-mantle boundary. From the results shown in Fig. 3 it is clear that at least in some places the LAB is not sharp but more gradual and that it is highly dependent on the tectonic and geodynamical conditions of the region. Regardless of the nature or the appearance of the LAB phase, lithospheric thickness was determined by picking the first negative peak below the depth of 50 km in the station stacked SRFs. This approach was chosen here in order to give the first approximation of the LAB depth under the Dinarides and later using the CCP stacks we explore the nature of the lithosphere-asthenosphere boundary in more detail.

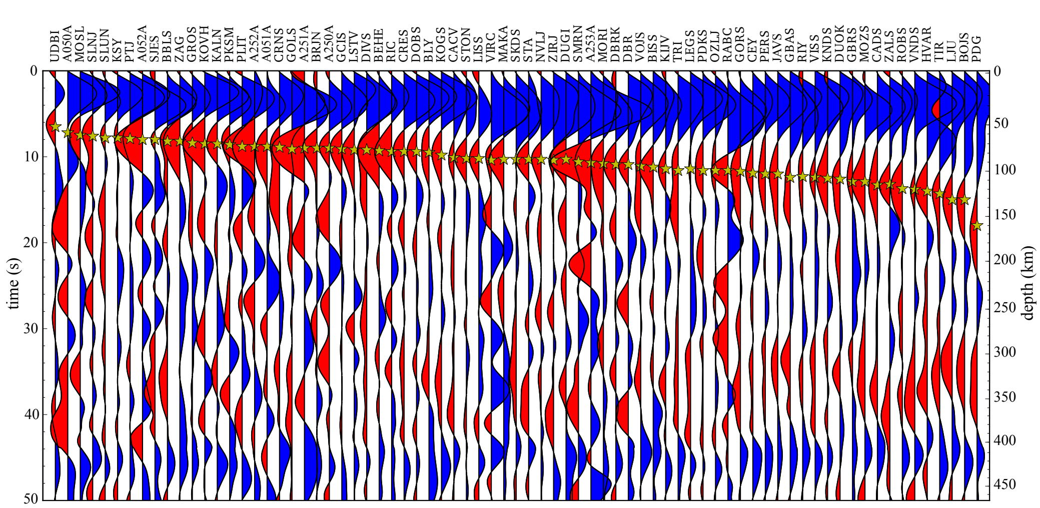

Figure 3: Depth converted SRF stacks from all stations sorted by the LAB depth. Yellow stars mark the automatically picked LAB depth at each individual station. Consistently positive signal at the end of the stacks corresponds to the 410 km discontinuity. Station names are given above each stack.

After the automatic picking, results were manually revised and, with the exception of station A050A, all picked depths were retained. At A050A (Fig.1) automatic picker found shallow low amplitude negative phase corresponding to conversion depth of 60 km. During manual revision we established this phase pick to be ambiguous as there is a strong high amplitude signal at around 160 km depth. The region around the A050A station is seen in some of the body wave tomographic images (Wortel, 2000; Piromallo and Morelli, 2003; Koulakov et al., 2009) as the area where a slab-gap in the Northern Dinarides ends, and a high velocity body, interpreted as a shallow slab or lithospheric underthrusting, starts to re-appear and continues south-eastwards all the way to the Hellenides. In addition, there is no other station in close proximity to A050A station to corroborate either of the two results. Therefore, we decided to leave both results as equally plausible (Fig. 4).

While performing manual revision of the automatically picked LAB depths a quality factor was assigned to each of the station SRF stacks. Our quality factor is similar to the one used by Miller and Piana Agostinetti (2012) and ranges from 1 to 5 (best-to-worst). The quality of station stack was attributed depending on the SRF appearance, using the following guidelines: (1) quality 1 to stations with one sharp positive phase (SMp converted phase from Moho) and one (or two) clear negative phases in the 50-200 km depth interval; (2) quality 2 to stations where positive phase is clearly observable, negative phase is wider or with some small contamination; (3) quality 3 to stations with a noticeable contamination on positive and negative phases, phase picking is complex but there is large number of usable SRFs; (4) quality 4 to stations with a noticeable contamination on positive and negative phases, phase picking is complex and there is small number of usable SRFs; (5) quality 5 to stations with strong contamination on the positive phase, where negative phase is not unique and visible and number of usable SRFs is small. Only one station was assigned quality 5 (SISC) and this station was excluded from further analysis and from all figures.

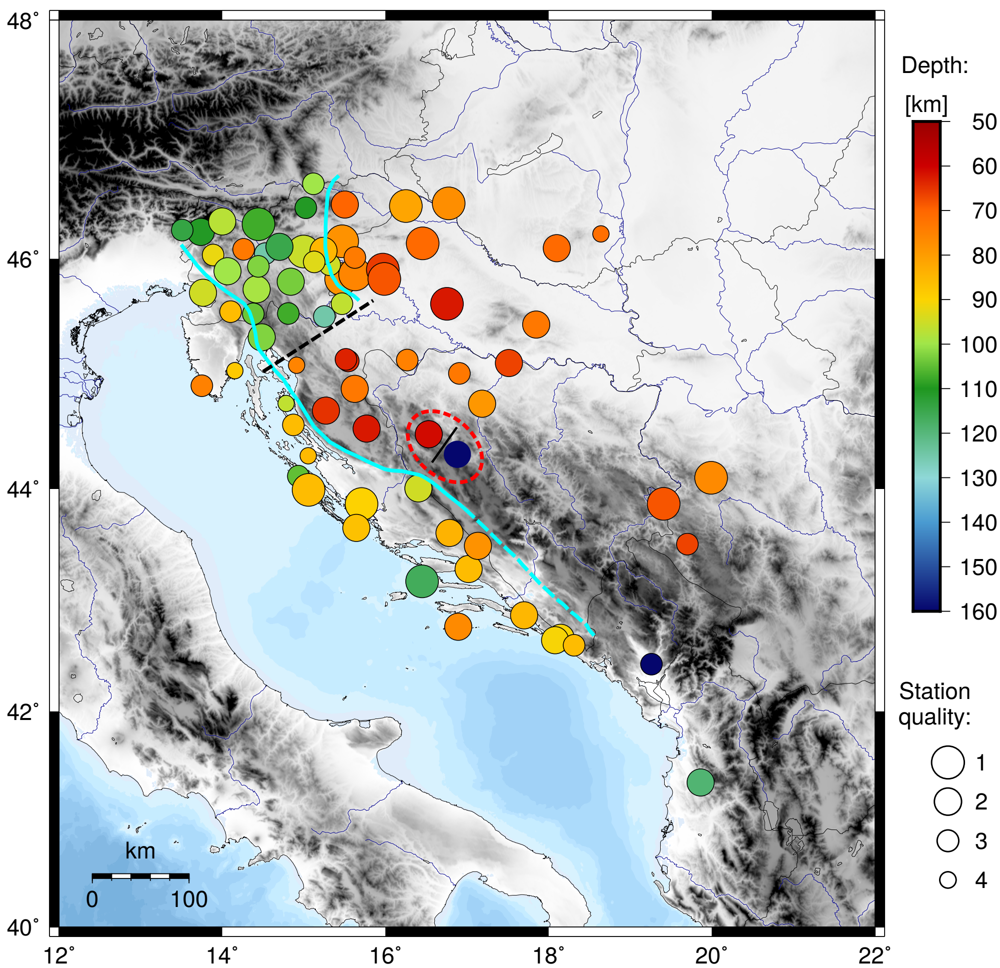

Figure 4: Map of the estimated depth of the lithosphere–asthenosphere boundary beneath the Dinarides and the surrounding areas. The symbol radius is scaled by the station quality (see text for details). The bluish lines mark the boundaries between regions with substantially different LAB depth values. Station A050A is enclosed within red dashed lines and both inferred LAB thickness results are drawn (see text). Dashed black line marks the approximate boundary between areas of thicker lithosphere under the NW Dinarides and thinned lithosphere under the Lika region.

Picked LAB depths range from 50 km found at the stations located in the region between the north-western and central Dinarides to more than 150 km at the station PDG in the southern Dinarides (Fig. 4). In the northernmost part of the investigated area there is a clear division into three distinct lithospheric thickness domains (outlined with blue lines in Fig. 4). In the whole Adriatic domain which roughly encompasses the eastern Adriatic coast and nearby hinterland area, LAB depths range mostly between 80 and 90 km. Crossing from the Adriatic domain into the NW Dinarides area estimated LAB depths change to around 100-120 km. Contrary to the LAB variation between Adriatic and NW Dinarides where a gradual transition to greater depths is observed, in the contact zone between the Dinarides and the western Pannonian basin the lithospheric thickness changes rapidly to much smaller values of around 70 km. The variations across the NW Dinarides are imaged on two profiles, BB' and CC' (Fig. 1), which start at the Adriatic coast and go over the NW Dinarides into the western margin of the Pannonian basin. In Fig. 5 we show the depth converted station stacked SRFs along these two profiles. The results in the profile BB' clearly image a more gradual transition between the lithosphere and the asthenosphere until about 150 km distance along the profile. The LAB zone in that portion of the profile is more spread in depth with two distinct peaks. From that point onward the LAB somewhat deepens, becomes sharper and only at the last station on the profile (GROS) the lithospheric thickness again is less than 100 km. Lack of clear delineation between different tectonic units along this profile is not unexpected as the profile BB' lies close to the triple junction between the Alps, Adria and Pannonia where the distinction between units becomes fuzzy. In the profile CC' the imaged LAB is continuous with clearly defined boundaries between different tectonic units. In the western part of the profile the LAB depths vary between 70 and 80 km and change to about 100 km as the profile crosses into the NW Dinarides at the distance of about 90 km.

This change in depth is more pronounced than in the profile BB' and most likely marks the beginning of the plate underthrusting at the base of the lithosphere. The lithosphere thickness of around 100 km persists and deepens to about 130 km in the central part of the profile where we see an abrupt jump back to lower values of 90-100 km. After this point the LAB zone becomes much sharper and better defined with additional reduction in lithospheric thickness levelling off to about 70 km at the western end of the Panonnian basin. One interesting result visible in the western and central parts of the profiles BB' and CC' is the later arriving negative amplitude signal (gray shaded zone in Fig. 5). Bianchi et al. (2014) also noticed a similar signal in their profile DD' just north of our profile BB'. We speculate that the source of this late negative amplitude signal is the sunken European slab leftover from the Alpine subduction (Handy et al., 2015).

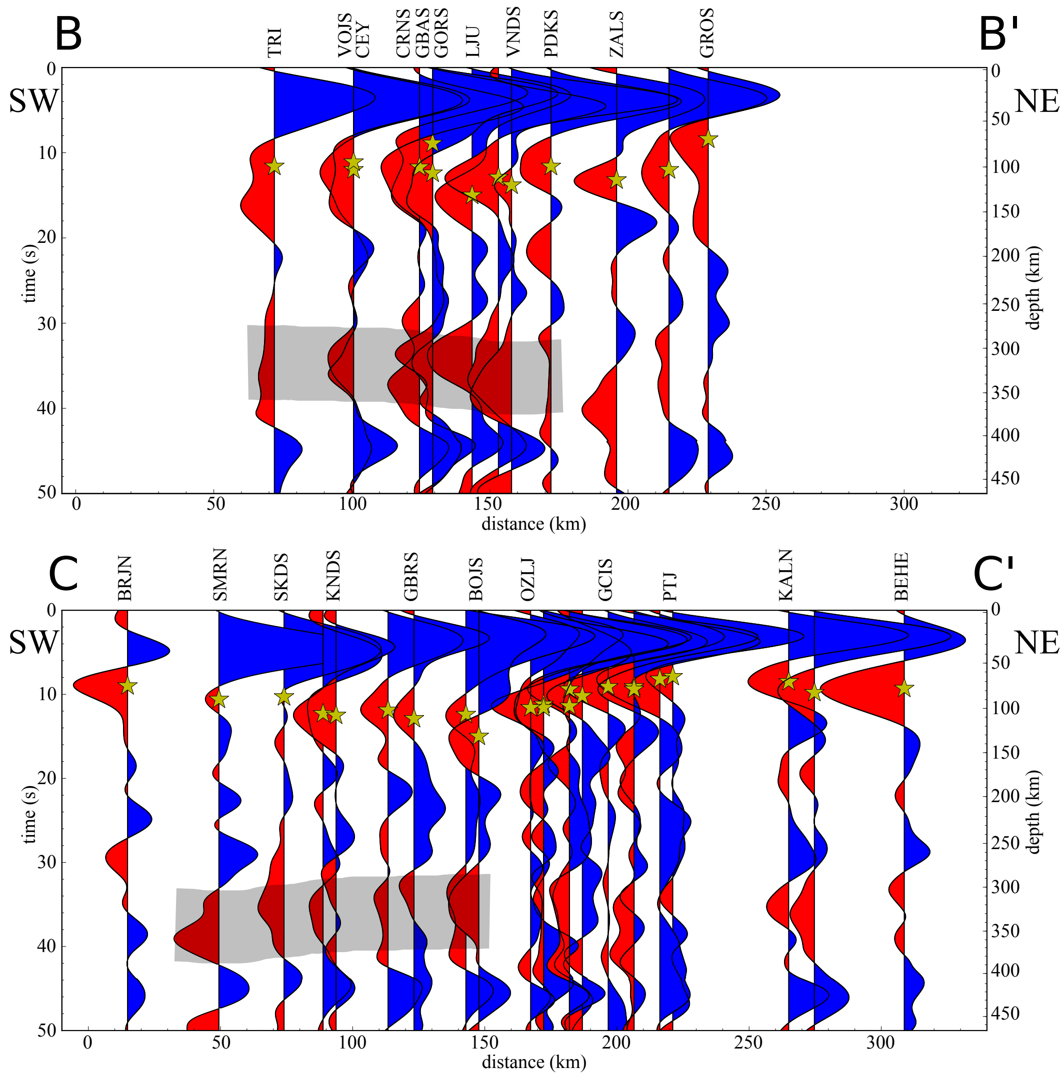

Figure 5: SRF station stacks along the profiles BB' and CC' (see Fig. 1 for location). All stations within 40 km distance from the profile are included. Yellow stars indicate picked LAB depths. For reference some of the station names are indicated above the SRF stacks. Gray masked area marks the deeper zone of low velocity just above the mantle transition zone.

Heading down south to the central part of the investigated area there is a major change in the LAB depth layout. In this zone, when compared with the northern section, the main difference is the lack of the deep lithospheric root under the Dinarides (area of Lika in Fig. 1 and Fig. 8). Instead, the results point to a severely thinned lithosphere under the Lika region with the possibility that this anomalous setup extends even further south to the central Dinarides (Fig. 4). In the coastal area of this region (i.e. the Adriatic domain) the results image the LAB depths between 90-100 km while the values under the Dinarides reach about 60 to 70 km with the same LAB depths continuing into the central part of the Panonnian basin. This is best seen in the station stacks along the profile DD' crossing this region (Fig. 6). The results image a transition from the area of a broad but well defined 90 km deep LAB to an area of thinned lithosphere lacking any of the properties seen under the NW Dinarides. On the other hand station stack estimates along the profile EE' laying just south of the profile DD' again show markedly different lithospheric and upper mantle structure layout. Along the western end of the profile EE' we observe the LAB at depths of 90 km which further enhances the notion of structural similarity of the whole Adriatic domain. In the central part of the profile around the station KIJV there is a slight deepening of the LAB to 100 km depth and then at the station A050A the phase associated with the LAB splits into two branches (green dotted line in Fig. 6). One branch shallows out to about 60 km and the second one deepens to about 160 km. The two branches are separated by the strong positive amplitude signal that can be traced along the profile (black dashed line in Fig. 6).

In the southern Dinarides our station coverage is limited with most of the stations located close to the Adriatic coast and only few stations laying further inland (Fig. 1). Similarly to the previously discussed subregions there is a clear continuation of the Adriatic domain in the south. LAB depths in this domain range between 85 and 95 km with the exception of the island station HVAR were we map LAB depth of 120 km. Unfortunately, due to the poor station coverage in southern Dinarides we can not be sure how far inland does the Adriatic domain extend in this region (see upper panel in Fig. 8). At the one station located somewhat further inland (PDG) near the southern tip of the Dinarides we observe exceptionally late negative amplitude phase indicating the LAB depth of about 160 km. These results may imply that in the southern Dinarides deformation front at the base of the lithosphere lies close to the coastline with a large jump in LAB depth at the transition from the Adriatic domain to the Dinarides. Furthermore, measurements at only three stations (DIVS, BBLS and SJES) in this region located further inland in the internal Dinarides show thinner lithosphere with thickness of about 70-80 km (Fig. 4).

Besides the negative LAB phases station stacks in Fig. 3 show several other consistent and characteristic phases. The most visible is the clear, shallow, positive phase we associate with the crust-mantle transition i.e. the Mohorovičić discontinuity (Moho). Moho depth estimates range between 25 and 50 km and agree well with the measurements from previous investigations (Skoko et al., 1987; Šumanovac et al., 2009; Stipčević et al., 2011). The second positive signal present on almost all the stations originates from the much deeper interface located at the depths between 400 and 430 km. This signal marks the beginning of the mantle transition zone which is usually associated with the olivine phase transition (Bina and Helffrich, 1994; Helffrich, 2000). The consistency of these signals along with the well defined LAB signal demonstrates the stability and reliability of the calculated S receiver functions.

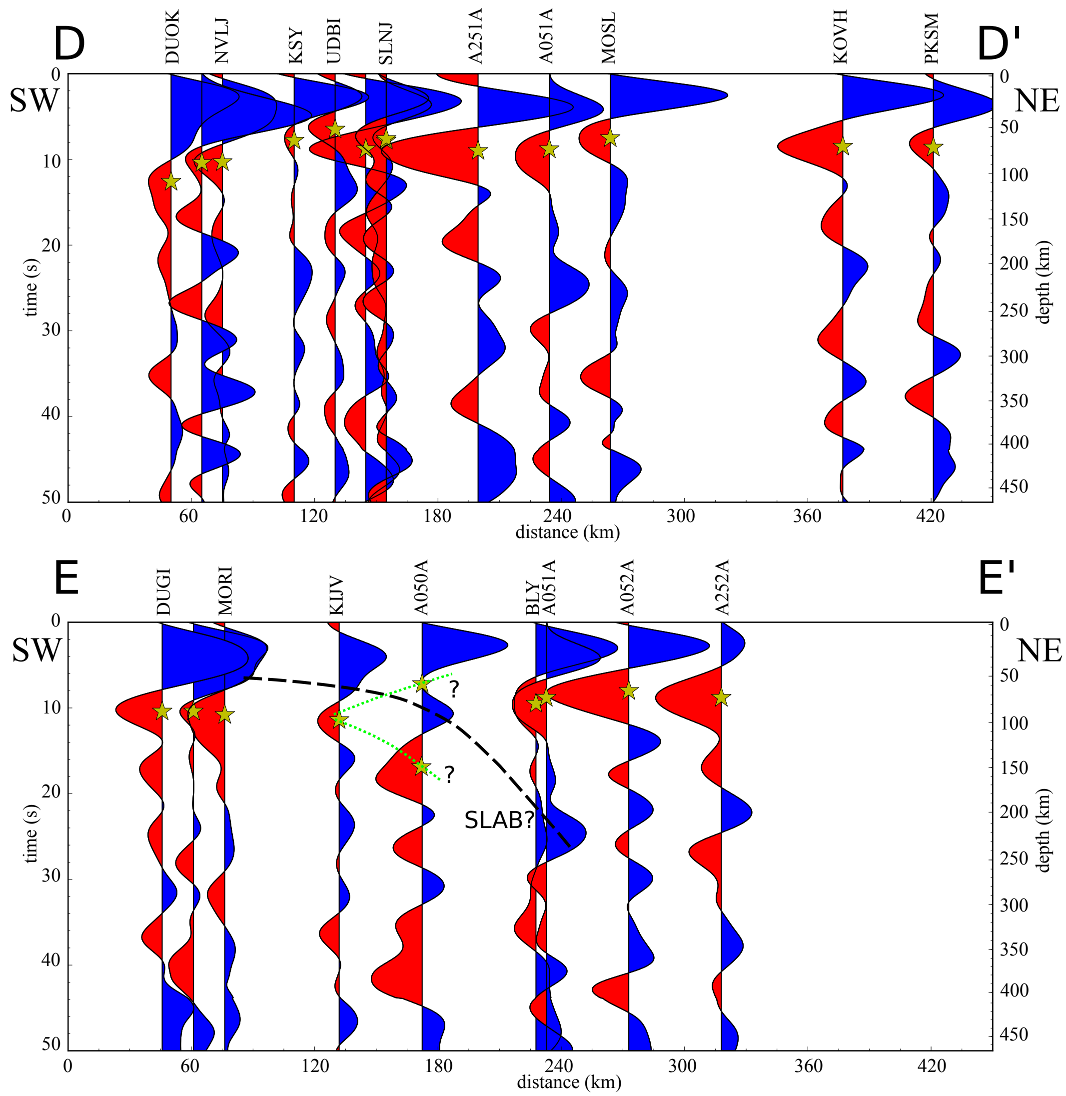

Figure 6: SRF station stacks along profiles DD' and EE' (see Fig. 1 for location). All stations within 40 km distance from the profile are included. Yellow stars indicate picked LAB depths. For reference some of the station names are indicated above the SRF stacks. At A050A station there are two possible LAB depths, hence the question marks. Dotted green lines mark two possible branches of the LAB depths. Dashed black line marks possible signal from the underthrusted Adriatic lithosphere.

4. Discussion

Dinarides are usually seen as the continuous unit divided into internal and external parts that developed in the wake of the collision process between Adria and European mainland (e.g. Tari and Pamić 1998; Pamić et al. 1998; Schmid et al. 2008). Although this may be true at the crustal level, teleseismic tomography results (Wortel, 2000; Piromallo and Morelli, 2003; Koulakov et al., 2009; Mitterbauer et al., 2011) show that at the lithospheric level this is not completely accurate. Tomography maps shallow high velocity anomalies under the north-western and central-southern Dinarides with a clear transition zone of lower seismic velocity between those two realms (Wortel, 2000; Piromallo and Morelli, 2003; Koulakov et al., 2009). Fast anomalies have been associated with the down-going slabs while the intermediate zone has been described as the ”slab gap” and various models have been put forward to explain it (see e.g. Ustaszewski et al. 2008; Handy et al. 2015). On the other hand, using the body wave travel times recorded on a set of stations crossing this zone, Šumanovac and Dudjak (2016) image a high velocity body reaching 200 km depth in the area of the ”slab gap”. In this sense analysis of the S receiver functions is indispensable as it provides an alternative way to interpret lithospheric structure in a very complex geodynamical setting.

Our findings have much in common with tomographic images showing an abrupt change in the upper mantle structure beneath the zone connecting north-western and central Dinarides. Under the north-western Dinarides we map lithospheric thickness in range of 100-120 km tapering off towards the Pannnonian Basin and the Adriatic Sea (Fig. 3). This is in agreement with Bianchi et al. (2014) who detected a thicker lithosphere (100-110km) in the transition zone between the Southern and the Eastern Alps and the Dinarides. The belt of a relatively thick lithosphere under the Dinarides in our measurements extends from the contact zone with the Alps to the northern boundary of Lika region (black dotted line in Fig. 3). After that point there is a significant change in the upper mantle seismic structure both in terms of lithospheric thickness and the appearance of the SRFs. In the northern portion of the CCP section along the profile AA' (Fig. 7) the upper mantle is characterized by the strong broad negative amplitude signal which we interpret as the underthrusting of the continental Adriatic lithosphere under the Dinarides. The assumption about the underthrusting or shallow subduction of Adria under the north-western Dinarides is supported by the data shown in Fig. 5. In both cross-sections (BB' and CC') continuous signal associated with the LAB is confined to the upper 150km with no indication of the deeper reaching slab.

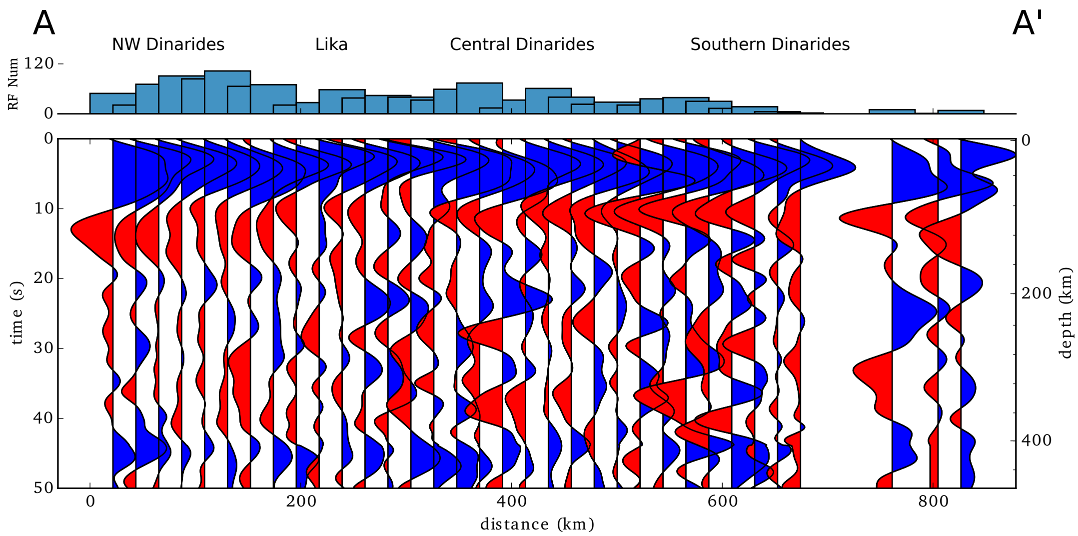

Figure 7: S receiver function CCP stacks along the profile AA' (see Fig. 1 for location). The receiver functions are binned in 40x80 km rectangular boxes along the profile where each box has a 50% overlap with the neighbouring boxes. All receiver functions with Sp90 piercing point locations within 40 km distance from the profile are included. The number of SRFs in each box is shown in the top panel and the locations of the main geographic regions are marked above this panel.

The most important and robust feature in our results is the clear contrast between the diffuse and shallow LAB beneath the Lika region and the well pronounced deeper LAB signal under the north-western and central Dinarides (Fig. 7). The results show a gradual decrease in the LAB sharpness and depth on the northern boundary of Lika while the transition towards central Dinarides is more dramatic with a step-like increase of about 30-40 km in LAB depth. Such a disposition of the LAB properties across the Dinarides leads us to hypothesize about the possible mechanisms explaining this zone of thin lithosphere zone in the Dinarides. Handy et al. (2015) have proposed an elegant solution combining shallow subduction in the Eastern Alps and northward movement of Adria as the driving mechanisms behind the thinning of the lithosphere in this area. In their model northward movement of Adria opened a gap in the lithosphere along the former Alpine-Dinaric transfer fault thus creating thin lithosphere zone under part of the Dinarides. Although this model gives valid explanation about the thicker lithosphere in the north-western Dinarides and lithospheric thinning under Lika region it does not provide details about the geodynamical setting under the central-south Dinarides and how it links with the northern section. Results of SRFs fit nicely in the framework proposed by Handy et al. (2015) but it is equally possible that lithospheric thinning may be the result of thermal erosion due to either a strong asthenospheric corner flow triggered by the sinking lithosphere at the north-western edge of the central Dinarides (Schefer et al., 2011; Matenco and Radivojević, 2012) or due to the inflow of hot asthenospheric material triggered by the spreading of the Pannonian basin (Ustaszewski et al., 2008). Interestingly, in contradiction to the model of Handy et al. (2015) the diffuse LAB under Lika region may imply small temperature gradient between mantle lithosphere and asthenosphere indicating slow thermal erosion as the source of the lithospheric thinning.

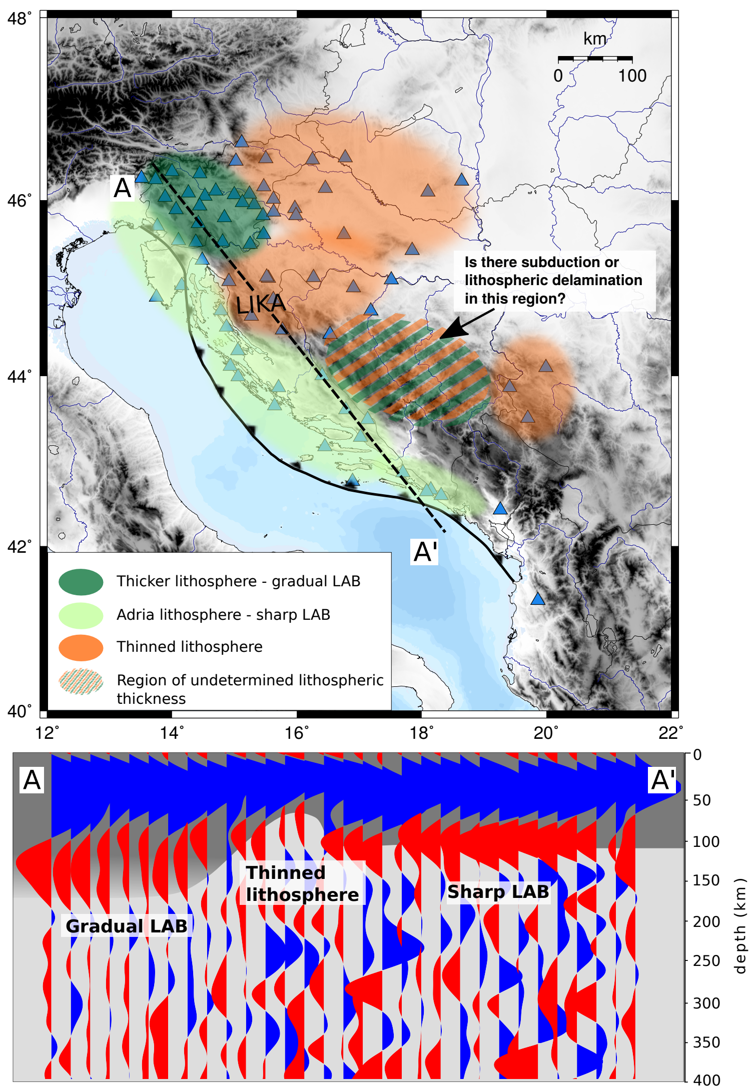

Figure 8: Upper panel is showing tectonic map of the wider Dinarides region with our main findings and the location of the main front thrust (black barbed line). Orange colour marks the regions with thinned lithosphere, dark green areas have thicker lithosphere and gradual LAB while light green colour marks the area underpinned with Adria derived lithosphere. The area marked with orange-green stripes is the region with undetermined LAB depth. LIKA - region with anomalously thin lithosphere (see text for details). Lower panel is showing sketch of the results along the profile AA' marked in the upper panel topped with SRF stacks shown in Fig. 7.

The existence of the upper mantle high velocity anomaly under the central-southern Dinarides has been established in a number of tomographic studies (Wortel, 2000; Piromallo and Morelli, 2003; Koulakov et al., 2009) and results shown in the cross-section EE' (Fig. 6) support this image. In the cross-section EE', starting at the Adriatic coast, there is a general broadening of the positive signal associated with the Moho that after station KIJV splits into two distinct pulses. After the split deeper positive signal can be traced on two more stations (A051A and BLY) laying deeper inland. This layout could be interpreted as the underthrusting in the External Dinarides which transforms to lithospheric delamination under the Internal Dinarides (black dashed line in Fig. 6). Moreover, at station A050A there are two negative amplitude signals that we may associate with the LAB (green dotted lines in Fig. 6). Shallower negative signal albeit small is important as it may signify the existence of the mantle wedge created by the lithospheric delamination while the deeper signal is much stronger and could mark the boundary between the sinking lithosphere and underlying asthenosphere.

As opposed to the northernmost part under the Central and the Southern Dinarides LAB is more prominent with a pulse like characteristics and is mostly confined to the narrow zone around 80-90 km depth (Fig. 7). Such a sharp and clear delineation implies not just thermally induced boundary but also a zone where the mechanically strong lithosphere transitions to the weaker asthenosphere. Pronounced LAB signal of comparable depth can be seen on most of the seismic stations along the eastern Adriatic coast and nearby hinterland area. This indicates structural similarity of the whole Adriatic area and points that, at least in the central Dinarides, the deformation front at the base of the lithosphere lies further inland (Fig. 8). Using the constraints from various geophysical datasets

Šumanovac (2015) places the lithospheric fault dividing the Adriatic and the Pannonian mantle underneath the central-southern External Dinarides at the northern edge of the seismically most active zone (see their Fig. 8). Unfortunately sparse data coverage in the central Dinarides (hatched area in Fig. 8) does not allow us to corroborate these findings and that will have to be addressed in future work.

In the southernmost part of the Dinarides only data from several stations which are located on or near the coast are available. Results here are comparable to those from the central Dinarides with the exception of the results from station PDG (Fig. 3). At that station data shows exceptionally deep LAB ($\sim$ 160 km) with the shallower duplicate positive signals which could be attributed to the double Moho thus indicating either still ongoing subduction (Bennett et al., 2008) or crustal thickening due to the underthrusting (e.g. Schmid et al. 2008). Three more stations (BBLS, DIVS, SJES) are located in the south-eastern part of the Internal Dinarides at the transition zone towards the South Carpathians and southeastern Pannonian Basin. Here we observe LAB depths between 70 and 80 km similar to the other areas in the contact zone between the Dinarides and the Pannonian Basin.

In the part of the Pannonian Basin encompassed by this study measured data shows relatively simple lithospheric structure with thin crust overlying sharp and shallow LAB. For the most part results point to lithospheric thickness in the range of 60-80 km slightly thickening towards the western edge of the basin. These measurements fit well with the overall image of the Pannonian Basin as the extensional structure and correlate well with the findings Geissler et al. (2010).

5. Conclusions

This study provides the first broad-scale measurement of the lithospheric thickness under the wider Dinarides area (Fig. 4). Negative amplitude signals in the S receiver functions are associated with the decrease in the seismic velocity and in this work we interpret the first significant negative amplitude in the depth range of 50-200km as the LAB. Furthermore, due to the dense distribution of the seismic stations and large number of usable S receiver functions we are able to map lateral depth variations of the LAB on the scale of several tens of kilometres. Our results show clear contrasts of the lithospheric structures between different parts of the Dinarides and the surrounding areas (Adriatic Sea and Pannonian Basin). The LAB beneath the NW Dinarides is deep (∼110 km) with gentle transition towards slightly shallower LAB under the Adriatic Sea and more abrupt transition towards significantly thinner lithosphere under the Lika region (∼50-60 km) and the Pannonian Basin (∼60-70 km). Shallow and diffuse LAB under the Lika region correlate well with the tomographic images showing low-velocity anomaly in the upper mantle of the north-central part of the Dinarides (Bijwaard and Spakman, 2000; Piromallo and Morelli, 2003; Koulakov et al., 2009). A pronounced LAB phase confined to the depths of 80-90 km can be traced along the whole central and southern portions the Dinarides enhancing the idea about rigid mechanical lithospheric block indenting deep into the mainland. Moreover, similar lithospheric structure is seen on all stations along the eastern Adriatic and nearby hinterland area indicating structural unity of the whole Adriatic domain (Fig. 8). Observation of the continuous positive signal in the Central Dinarides reaching depths of 200 km (profile EE' in Fig. 4) coincide with the teleseismic tomography results showing persistent upper mantle high velocity anomaly under this area.

Result shown in this work are the first step in establishing a framework of the lithospheric model describing the evolution of the Dinarides and their relationship with the surrounding tectonic provinces. In the future work we plan to incorporate results from different geophysical investigations and expand our analysis to include additional stations deployed in the course of AlpArray project (Molinari et al., 2016) and its CASE complementary experiment (Dasović et al., 2017).

Acknowledgments

The study has been fully supported by the Croatian Science Foundation, grant HRZZ IP 2014-09-9666. The data were collected by the Croatian Seismograph Network operated by the Seismological Survey of Republic of Croatia, the A. Mohorovičić Geophysical Institute, Slovenian Environment Agency (ARSO), Republic Hydrometeorological Service of Republic of Srpska (RHMZ RS), Geodetic and Geophysical Research Institute of the Hungarian Academy of Science (HU) and MedNet project partner institutions (MN). All support in collecting and storing seismic data is gratefully acknowledged. Operation of the stations CACV, KSY and STA is financed by the HEP group (Hrvatska elektroprivreda d.d.). The authors are grateful to the AlpArray Seismic Network Team who builds and maintains the entire AlpArray Seismic Network.

Reference

Abt, D.L., Fischer, K.M., French, S.W., Ford, H.A., Yuan, H., Romanowicz, B., 2010. North american lithospheric discontinuity structure imaged by ps and sp receiver functions. J. Geophys. Res. 115, B09301. doi:10.1029/2009JB006914.

Aljinović, B., 1983. Najdublji seizmički horizonti sjeveroistočnog Jadrana. Doctoral dissertation (in croatian). University of Zagreb, Faculty of Science.

Bennett, R.a., Hreinsdóttir, S., Buble, G., Bašić, T., Bačić, Ž., Marjanović, M., Casale, G., Gendaszek, A., Cowan, D., 2008. Eocene to present subduction of southern adria mantle lithosphere beneath the dinarides. Geology 36, 3. doi:10.1130/G24136A.1.

Bianchi, I., Miller, M.S., Bokelmann, G., 2014. Insights on the upper mantle beneath the eastern alps. Earth Planet. Sci. Lett. 403, 199–209. doi:10.1016/j.epsl.2014.06.051.

Bijwaard, H., Spakman, W., 2000. Non-linear global p -wave tomography by iterated linearized inversion. Geophys. J. Int. 141, 71–82. doi:10.1046/j.1365-246X.2000.00053.x.

Bina, C.R., Helffrich, G., 1994. Phase transition clapeyron slopes and transition zone seismic discontinuity topography. J. Geophys. Res. 99, 15853. doi:10.1029/94JB00462.

Brückl, E., Behm, M., Decker, K., Grad, M., Guterch, A., Keller, G.R., Thybo, H., 2010. Crustal structure and active tectonics in the eastern alps. Tectonics 29, n/a–n/a. doi:10.1029/2009TC002491.

Brückl, E., Bleibinhaus, F., Gosar, A., Grad, M., Guterch, A., Hrubcová, P., Keller, G.R., Majdański, M., Šumanovac, F., Tiira, T., Yliniemi, J., Hegedűs, E., Thybo, H., 2007. Crustal structure due to collisional and escape tectonics in the eastern alps region based on profiles alp01 and alp02 from the alp 2002 seismic experiment. J. Geophys. Res. 112, B06308. doi:10.1029/2006JB004687.

Dasović, I., Molinari, I., Stipčević, J., Šipka, V., Salimbeni, S., Jarić, D., Prevolnik, S., Kissling, E., Clinton, J., Giardini, D., Group, t.A.C.W., 2017. The alparray-case project: temporary broadband seismic network deployment and characterization, in: Geophys. Res. Abstr., pp. Vol. 19, EGU2017–13952–1.

Dueker, K.G., Sheehan, A.F., 1997. Mantle discontinuity structure from midpoint stacks of converted p to s waves across the yellowstone hotspot track. J. Geophys. Res. Solid Earth 102, 8313–8327. doi:10.1029/96JB03857.

Farra, V., Vinnik, L., 2000. Upper mantle stratification by p and s receiver functions. Geophys. J. Int. 141, 699–712. doi:10.1046/j.1365-246x.2000.00118.x.

Geissler, W.H., Kämpf, H., Skácelová, Z., Plomerová, J., Babuška, V., Kind, R., 2012. Lithosphere structure of the ne bohemian massif (sudetes) — a teleseismic receiver function study. Tectonophysics 564-565, 12–37. doi:10.1016/j.tecto.2012.05.005.

Geissler, W.H., Sodoudi, F., Kind, R., 2010. Thickness of the central and eastern european lithosphere as seen by s receiver functions. Geophys. J. Int. 181, 604–634. doi:10.1111/j.1365-246X.2010.04548.x.

Handy, M.R., Ustaszewski, K., Kissling, E., 2015. Reconstructing the alps–carpathians–dinarides as a key to understanding switches in subduction polarity, slab gaps and surface motion. Int. J. Earth Sci. 104, 1–26. doi:10.1007/s00531-014-1060-3.

Helffrich, G., 2000. Topography of the transition zone seismic discontinuities. Rev. Geophys. 38, 141–158. doi:10.1029/1999RG000060.

Kennett, B.L.N., 1991. The removal of free surface interactions from three-component seismograms. Geophys. J. Int. 104, 153–154. doi:10.1111/j.1365-246X.1991.tb02501.x.

Kind, R., Yuan, X., Kumar, P., 2012. Seismic receiver functions and the lithosphere–asthenosphere boundary. Tectonophysics 536-537, 25–43. doi:10.1016/j.tecto.2012.03.005.

Koulakov, I., Kaban, M.K., Tesauro, M., Cloetingh, S., 2009. P - and s - velocity anomalies in the upper mantle beneath europe from tomographic inversion of isc data. Geophys. J. Int. 179, 345–366. doi:10.1111/j.1365-246X.2009.04279.x.

Levander, A., Miller, M.S., 2012. Evolutionary aspects of lithosphere discontinuity structure in the western u.s. Geochemistry, Geophys. Geosystems 13, Q0AK07. doi:10.1029/2012GC004056.

Ligorría, J.P., Ammon, C.J., 1999. Iterative deconvolution and receiver function estimation. Bull. Seismol. Soc. Am. 89, 1395–1400.

Lippitsch, R., 2003. Upper mantle structure beneath the alpine orogen from high-resolution teleseismic tomography. J. Geophys. Res. 108, 2376. doi:10.1029/2002JB002016.

Matenco, L., Radivojević, D., 2012. On the formation and evolution of the pannonian basin: Constraints derived from the structure of the junction area between the carpathians and dinarides. Tectonics 31, n/a–n/a. doi:10.1029/2012TC003206.

Miller, M.S., Eaton, D.W., 2010. Formation of cratonic mantle keels by arc accretion: Evidence from s receiver functions. Geophys. Res. Lett. 37, n/a–n/a. doi:10.1029/2010GL044366.

Miller, M.S., Piana Agostinetti, N., 2012. Insights into the evolution of the italian lithospheric structure from s receiver function analysis. Earth Planet. Sci. Lett. 345-348, 49–59. doi:10.1016/j.epsl.2012.06.028.

Mitterbauer, U., Behm, M., Brückl, E., Lippitsch, R., Guterch, A., Keller, G.R., Koslovskaya, E., Rumpfhuber, E.M., Šumanovac, F., 2011. Shape and origin of the east-alpine slab constrained by the alpass teleseismic model. Tectonophysics 510, 195–206. doi:10.1016/j.tecto.2011.07.001.

Molinari, I., Clinton, J., Kissling, E., Hetényi, G., Giardini, D., Stipčević, J., Dasović, I., Herak, M., Šipka, V., Wéber, Z., Gráczer, Z., Solarino, S., 2016. Swiss-alparray temporary broadband seismic stations deployment and noise characterization. Adv. Geosci. 43, 15–29. doi:10.5194/adgeo-43-15-2016.

Neubauer, F., 2014. The structure of the eastern alps: From eduard suess to present-day knowledge. Austrian J. Earth Sci. 107, 83–93.

Pamić, J., 2002. The sava-vardar zone of the dinarides and hellenides versus the vardar ocean. Eclogae Geol. Helv. 95, 99–113.

Pamić, J., Gušić, I., Jelaska, V., 1998. Geodynamic evolution of the central dinarides. Tectonophysics 297, 251–268. doi:10.1016/S0040-1951(98)00171-1.

Piromallo, C., Morelli, A., 2003. P wave tomography of the mantle under the alpine-mediterranean area. J. Geophys. Res. Solid Earth 108, 2065. doi:10.1029/2002JB001757.

Ratschbacher, L., Frisch, W., Linzer, H.G., Merle, O., 1991a. Lateral extrusion in the eastern alps, part 2: Structural analysis. Tectonics 10, 257–271. doi:10.1029/90TC02623.

Ratschbacher, L., Merle, O., Davy, P., Cobbold, P., 1991b. Lateral extrusion in the eastern alps, part 1: Boundary conditions and experiments scaled for gravity. Tectonics 10, 245–256. doi:10.1029/90TC02622.

Schefer, S., Cvetković, V., Fügenschuh, B., Kounov, A., Ovtcharova, M., Schaltegger, U., Schmid, S.M., 2011. Cenozoic granitoids in the dinarides of southern serbia: age of intrusion, isotope geochemistry, exhumation history and significance for the geodynamic evolution of the balkan peninsula. Int. J. Earth Sci. 100, 1181–1206. doi:10.1007/s00531-010-0599-x.

Schmid, S.M., Bernoulli, D., Fügenschuh, B., Matenco, L., Schefer, S., Schuster, R., Tischler, M., Ustaszewski, K., 2008. The alpine-carpathian-dinaridic orogenic system: correlation and evolution of tectonic units. Swiss J. Geosci. 101, 139–183. doi:10.1007/s00015-008-1247-3.

Shen, X., Liu, M., Gao, Y., Wang, W., Shi, Y., An, M., Zhang, Y., Liu, X., 2017. Lithospheric structure across the northeastern margin of the tibetan plateau: Implications for the plateau's lateral growth. Earth Planet. Sci. Lett. 459, 80–92. doi:10.1016/j.epsl.2016.11.027.

Skoko, D., Prelogovič, E., Alinovič, B., 1987. Geological structure of the earth's crust above the moho discontinuity in yugoslavia. Geophys. J. Int. 89, 379–382. doi:10.1111/j.1365-246X.1987.tb04434.x.

Stipčević, J., Tkalčić, H., Herak, M., Markušić, S., Herak, D., 2011. Crustal and uppermost mantle structure beneath the external dinarides, croatia, determined from teleseismic receiver functions. Geophys. J. Int. 185, 1103–1119. doi:10.1111/j.1365-246X.2011.05004.x.

Šumanovac, F., 2015. Lithosphere model of the pannonian–adriatic overthrusting. Tectonophysics 665, 79–91. doi:10.1016/j.tecto.2015.09.032.

Šumanovac, F., Dudjak, D., 2016. Descending lithosphere slab beneath the northwest dinarides from teleseismic tomography. J. Geodyn. 102, 171–184. doi:10.1016/j.jog.2016.09.007.

Šumanovac, F., Orešković, J., Grad, M., 2009. Crustal structure at the contact of the dinarides and pannonian basin based on 2-d seismic and gravity interpretation of the alp07 profile in the alp 2002 experiment. Geophys. J. Int. 179, 615–633. doi:10.1111/j.1365-246X.2009.04288.x.

Tari, V., Pamić, J., 1998. Geodynamic evolution of the northern dinarides and the southern part of the pannonian basin. Tectonophysics 297, 269–281. doi:10.1016/S0040-1951(98)00172-3.

Ustaszewski, K., Kounov, A., Schmid, S.M., Schaltegger, U., Krenn, E., Frank, W., Fügenschuh, B., 2010. Evolution of the adria-europe plate boundary in the northern dinarides: From continent-continent collision to back-arc extension. Tectonics 29, TC6017. doi:10.1029/2010TC002668.

Ustaszewski, K., Schmid, S.M., Fügenschuh, B., Tischler, M., Kissling, E., Spakman, W., 2008. A map-view restoration of the alpine-carpathian-dinaridic system for the early miocene. Swiss J. Geosci. 101, 273–294. doi:10.1007/s00015-008-1288-7.

Wilson, D.C., Angus, D.A., Ni, J.F., Grand, S.P., 2006. Constraints on the interpretation of s -to- p receiver functions. Geophys. J. Int. 165, 969–980. doi:10.1111/j.1365-246X.2006.02981.x.

Wortel, M.J.R., 2000. Subduction and slab detachment in the mediterranean-carpathian region. Science (80-.). 290, 1910–1917. doi:10.1126/science.290.5498.1910.

Yang, X., Pavlis, G.L., Wang, Y., 2016. A quality control method for teleseismic p wave receiver functions. Bull. Seismol. Soc. Am. 106, 1948–1962. doi:10.1785/0120150347.

Yuan, X., Kind, R., Li, X., Wang, R., 2006. The s receiver functions: synthetics and data example. Geophys. J. Int. 165, 555–564. doi:10.1111/j.1365-246X.2006.02885.x.

Zhai, Y., Levander, A., 2011. Receiver function imaging in strongly laterally heterogeneous crust: Synthetic modeling of bolivar data. Earthq. Sci. 24, 45–54. doi:10.1007/s11589-011-0768-4.